Lab on a Chip

Microfluidic desalination techniques and their potential applications†

S. H. Roelofs,[*a] **A. van den Berg,**[a‡] **and M. Odijk**[a]

In this review we discuss recent developments in the emerging research field of miniaturized desalination. Traditionally desalination is performed to convert salt water into potable water and research is focused on improving performance of large-scale desalination plants. Microfluidic desalination offers several new opportunities in comparison to macro-scale desalination, such as providing a platform to increase fundamental knowledge of ion transport on the nano- and microfluidic scale and new microfluidic sample preparation methods. This approach has also lead to the development of new desalination techniques, based on micro/nanofluidic ion-transport phenomena, which are potential candidates for up-scaling to (portable) drinking water devices. This review assesses microfluidic desalination techniques on their applications and is meant to contribute to further implementation of microfluidic desalination techniques in the lab-on-chip community.

1 Introduction

Macrofluidic desalination techniques are established methods for drinking water production from salt water and are frequently highlighted as a contributing solution to reducing the world-wide drinking water shortage[1–3]. In contrast, microfluidic desalination is an emerging research field, which serves as an optimizing tool for traditional techniques and offers new opportunities for lab-on-chip devices.

This literature review focuses on desalination on the micro- and nanofluidic scale and it's potential applications. This is further defined as devices/setups with two dimensions in the sub-mm scale and flow rates in the order of nano- to microliter per minute. The trend of down-scaling medical analysis to a lab-on-chip format has created new application areas for desalination, mainly as tool in sample preparation. Advantages of online sample desalination in contrast to manual offline methods include speed of operation, improved reproducibility and reduction of dead volume, sample loss and contamination. The terms on- and offline are both frequently used in the field of analytical chemistry. The term "offline" refers to a discontinuous process in which each manipulation is performed subsequently, whereas in an "online" process the individual steps are connected via continuous flow and are performed in a single pass. Besides this, desalination-on-chip can contribute to the understanding of ion transport in existing large-scale desalination devices and hence improve performance (e.g. desalination percentage and regeneration speed). In this review

the operational principle of each technique is described, followed by a discussion on promising application areas. The following techniques are considered: dialysis, electrodialysis (ED), (membrane) capacitive deionization ((M)CDI), ion concentration polarization (ICP), and electrochemical desalination. Concentration techniques such as solid phase extraction (SPE)[4,5], ion exchange columns and separation techniques for compounds of interests such as liquid chromatography (LC)[6], isotachiophoresis (ITP)[7] and electrophoresis[5] have been reviewed recently and are therefore not considered.

The content of the review is structured in the following manner. In section 3 an overview is given of established macro-scale desalination techniques for later comparison. In section 4 microfluidic desalination techniques are discussed based on their specifications and applications.

2 Theory

Before progressing reviewing the microfluidic desalination techniques, a quick introduction into the relevant terms and operational mechanisms that are essential in characterizing and classifying desalination techniques is given.

2.1 Electrical double layer

The occurrence of a double layer is a phenomena that is found at the interface of a conductor and an electrolyte[8], where the surface charge of the conductor is screened in the liquid through a distribution profile of ions. This phenomena can be used to store ions. Methods to model the distribution of ions in the double layer were reviewed by Burt et al.[9]. Helmholtz

a BIOS - the Lab-on-a-Chip group, Mesa+ Institute for Nanotechnology, MIRA Institute, University of Twente, P.O. box 217, 7500 AE Enschede, The Netherlands, E-mail: s.h.roelofs@utwente.nl

was the first to introduce a double layer model in the 19th century[10,11], in which he considered a single layer of solvated ions in the solution packed in close proximity to an electrode. The compact layer was also referred to as Helmholtz layer. Gouy and Chapman[12] extended the double layer model with the contribution of mobile of ions in solution, in close proximity to the electrode. This results in a double layer which is made up of a compact layer of ions packed to the surface together with a distribution profile of ions which extends into the solution. Stern[13] combined the two models and formulated the widely accepted Gouy-Chapman-Stern (GCS) theory.

2.2 Double layer overlap

A category of desalination techniques relies on the utilization of nanopores. Within the pores, double layer overlap occurs if the width of the pores is in the same size range as the Debye length, see figure 4. Figure 4a represents a pore in which no double layer overlap occurs. In this situation, the channel is much wider than the Debye length. The Debye length is a characteristic length indicating the distance of the diffuse layer into the solution. Typical values are 1 to 10 nm for concentrations of 100 to 1 mM. The potential is maximum close to the surface and zero at the center of the pore. The concentration of counter-ions is higher than the concentration of co-ions. Figure 4b explains the phenomena of double layer overlap. The potential does not reach zero in the center of the pore and the co-ion presence in the pore is nihil[14,15].

2.3 Performance indicators

A frequently mentioned performance indicator for desalination is the water recovery rate, which is the ratio of fresh water produced over the influent solution and can be calculated from:

$$recovery\% = \frac{flowrate\ fresh\ water\ produced}{flowrate\ influent\ stream} \times 100 \quad (1)$$

For large scale desalination energy efficiency is a key performance parameter. For microfluidic applications this is of minor importance, because the energy consumption is generally low, for a complete theoretical overview the minimum energy required for desalination is described in this paragraph. The minimum amount of energy that is required to remove ions from the solution is equal to the amount of energy that can be gained from mixing the fresh and concentrated stream. The term Gibbs free energy (G [J mol^{-1}]) indicates the amount of energy in a system available for work[16,17]. The energy required to desalinate a salt solution is given by the change in Gibbs energy (ΔG) of the solutions before and after desalination according to,

$$\Delta G = G_d + G_c - G_{in} \quad (2)$$

where G_d, G_c and G_i are respectively the Gibbs free energy of the desalinated, concentrated brine, and influent stream. The Gibbs free energy of species i in a solution is proportional to the chemical potential (μ_i) and the number of ions (n_i) in a solution, according to $G = \sum \mu_i n_i$[16]. The chemical potential of component i in a solution is given by,

$$\mu_i = \mu_i^0 + RT \ln x_i \gamma_i \quad (3)$$

where x_i is the mole fraction of species i in the solution and γ_i is the corresponding activity coefficient. The activity coefficient is a dimensionless number which accounts for the ion-ion interaction in the liquid. For an ideal solution, in which there is no ion-ion interaction, the activity coefficient is 1[17]. The minimum amount of energy required to desalinate water is expressed through[17],

$$\Delta G = \sum_i [c_{i,d} V_d RT \ln(x_{i,d} \gamma_{i,d}) + c_{i,c} V_c RT \ln(x_{i,c} \gamma_{i,c}) -$$
$$c_{i,in} V_{in} RT \ln(x_{i,in} \gamma_{i,in})] \quad (4)$$

where the concentration of the desalinated, concentrated and influent water streams are represented by $c_{i,d}$, $c_{i,c}$ and $c_{i,in}$, respectively. V_d, V_c and V_{in} refer to the volumes of the corresponding three water streams. The minimum amount of energy needed to desalinate water depends on the concentration of the influent and effluent streams. For brackish water desalination, the theoretical minimum is around 0.17 kWh m^{-3} for the case where the input concentration is twice the output concentration[18]. The total energy consumption of a desalination plant is higher than the theoretical minimum and includes the energy consumption of pumps, valves and losses due to friction.

3 Traditional desalination methods

Desalination of water is typically applied on the macro-scale for drinking water production from seawater or brackish water. The salinity of seawater is 35 g/L on average[19], while brackish water has a salinity of ≈ 1-10 g/L[20]. Drinking water is also known as potable water and typically has a salinity < 1000 mg L^{-1}[20]. According to the World Health Organisation, the amount of people living in countries suffering from a fresh water shortage is expected to increase from one-third of the world's population (2004) to two-thirds in 2025[21,22]. The urge for energy efficient methods to unlock the salt water sources for drinking water supply is reflected in the growth of the amount of desalination plants throughout the world in the
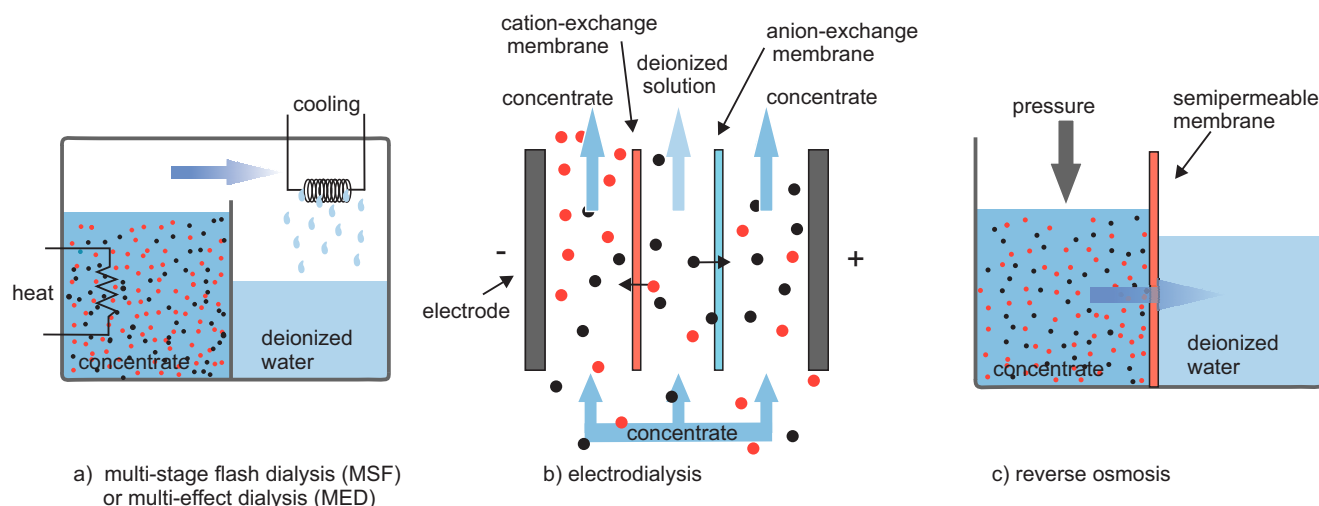
Fig. 1 Overview of basic principles of desalination techniques commonly applied for seawater desalination: a) Multi stage flash distillation (MSF) and multi-effect distillation (MED), where heat is used to distill salt water and the condensate is collected. b) An electrodialysis system, which consists of two electrodes with alternating cat- and anion exchange membranes are placed in parallel[24]. The elements are separated through spacers. A potential is applied across the stack. The ions in the electrolyte, entering from below, transport through the membranes. Cations can only pass through the cation selective membranes, whereas anions can only pass through anion selective membranes. The result is alternating dilute and concentrated streams. c) Reverse osmosis (RO) which is based on an over-pressure on the concentration side of a semipermeable membrane[25].

past decade[22,23]. The worldwide desalination capacity is expected to double in size between 2008 and 2016 to 38 billion m^3 per year[22].

An overview of commonly implemented techniques for seawater desalination is given in Fig. 1. Fig. 1a represents thermal desalination methods including multi-stage flash distillation (MSF) and multi-effect distillation (MED). Water is evaporated through the input of heat and condenses in a fresh water reservoir. Reverse osmosis (Fig. 1b) is a membrane based process. A pressure is applied to pass water molecules through a semi-permeable membrane, leaving ions behind in the concentrated reservoir. The typical recovery rate of RO varies from 35% to 85% depending on amongst others the concentration and composition of the feed solution[26]. According to Ghaffour et al. the typical energy consumption of a reverse osmosis desalination plant for seawater and brackish water is 3-4 and 0.5-2.5 kWh m^{-3}, respectively[3].

An alternative technique is electrodialysis (Fig. 1c). Alternating cat- and anion selective membranes are stacked. A potential is applied across the stack which causes the ions in the electrolyte to transport through the membranes until they are blocked. The result is alternating channels of fresh and concentrated water streams[18]. Thermal methods and reverse osmosis are energy intensive processes, due to either high temperatures (MSF, MED) or high pressures (RO). Currently RO is the most energy efficient method for desalination of seawater and therefore the most favored method for desalination

facilities build in the last two decades[22]. Electrodialysis is competitive in energy efficiency for desalination of brackish water[27] and reaches a recovery percentage of 94% in one cycle and 97% in two cycles[26]. The energy consumption of electrodialysis is 0.4-8.7 kWh m^{-3} according to AlMarzooqi et al.[28].

4 Microfluidic desalination techniques

The microfluidic desalination techniques are discussed in this section and our findings are summarized in two tables. Table 1 contains an overview of each of the techniques and can be used for comparison of the dimensions, flowrates and achieved desalination performance. For potable water production the energy efficiency is a critical parameter, while this is of minor importance for microfluidic desalination. A qualification for each technique, considering the applications, advantages and disadvantages is given in table 2.

4.1 Dialysis

Dialysis is a separation process based on selective diffusion of molecules and ions through a membrane. The salt concentration of the influent stream is diluted through the membrane into a second solvent with a low/zero salt concentration, whereas alternative described desalination techniques result in a concentrated brine solution and a dilute stream. The components to be removed diffuse across the membrane, traditionally
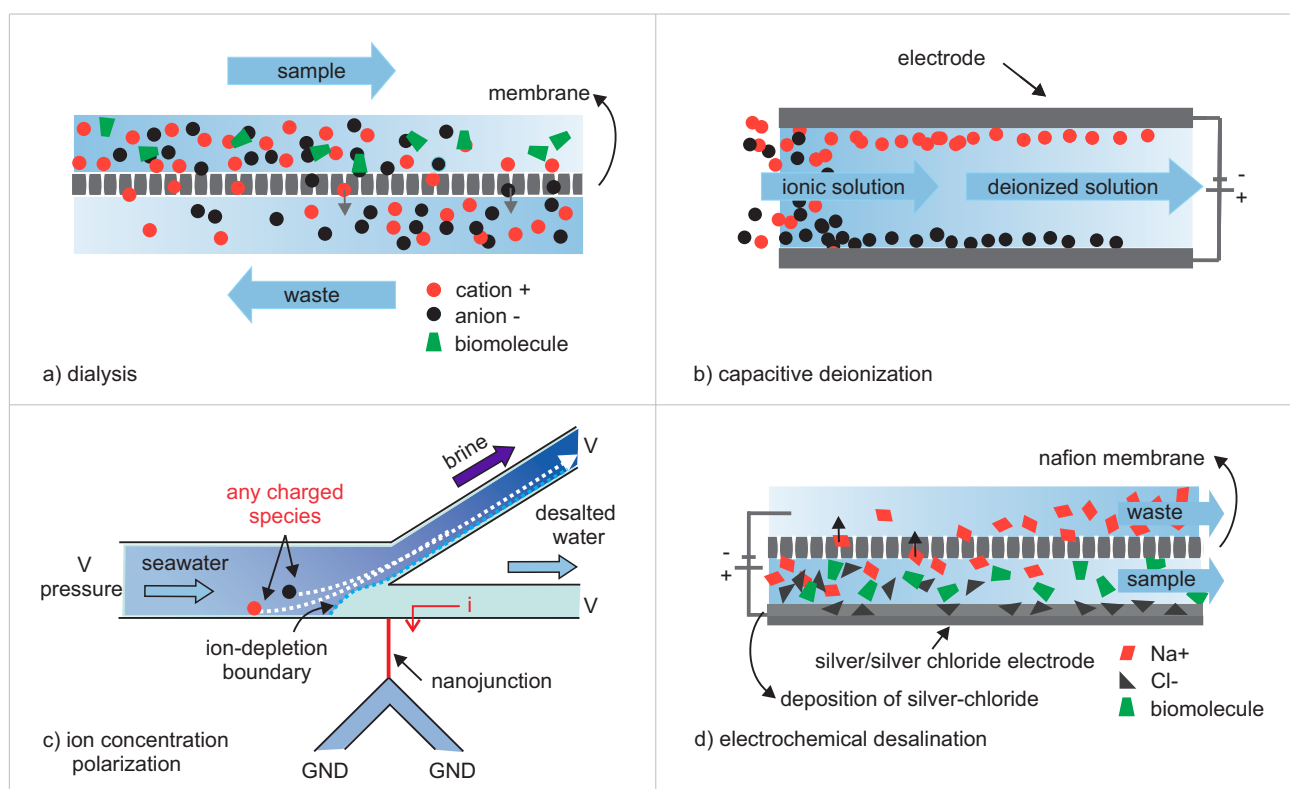
Fig. 2 Schematic of operational principle of microfluidic desalination techniques: a) Dialysis is a separation process based on the diffusion of ions through a membrane. The top channel contains a sample in a concentrated salt solution, and the bottom channel contains the waste stream. b) Capacitive deionization, which is based on the storage of ions in the electrical double layer of the electrodes upon the application of a potential of $\approx$1V. c) Ion concentration polarization is a phenomena that uses the formation of a depletion zone around a nanopore which is situated as a junction between two microfluidic channels with different potentials, modified from Kim et al.[29]. d) Electrochemical desalination is based on Faradaic reactions. Oxidation of silver at the Ag/AgCl electrode results in silver chloride formation. Na$^+$ ions pass through the nafion membrane[30].

fabricated from cellulose or poly(vinylidene fluoride)[31], into a buffer solution. The operational principle is illustrated by Fig. 2a. A sample is flowing in the top channel, and a buffer solution in the bottom channel. The channels are separated by a membrane, which separation characteristics are specified by a molecular weight cut-off number (MWCO). Generally the pore size is not specified but the MWCO number is provided in the papers cited. The compounds of interest remain in the top channel, while salts diffuse through the membrane to the bottom channel. Microdialysis has been implemented on-chip and coupled to electrospray ionization mass spectrometry systems (ESI-MS) as a sample preparation method[32,33]. Analysis of ESI-MS spectra from protein- or DNA-samples with a high concentration of buffers and salts can be impossible due to a low signal-to-noise ratio also known as ion suppression[34–37].

The development of miniaturized dialysis is focused on fabrication methods for membranes on-chip as well as increasing the speed of the process to enable online desalination in com-

bination with analysis techniques. The diffusion time, which can be calculated through $t_D \approx x^2/2D$, is shorter in microfluidic systems compared to larger dialysis devices. A decrease in width of the channel by a factor 10 leads to a decrease in the diffusion time of a factor 100. However, within dialysis systems on chip the diffusion time across membranes is often the limiting factor and therefore more relevant is the development of ultra-thin membranes on chip which achieve a significantly lower membrane diffusion time[38]. Zhang et al. studied the formation of free standing films in a microfluidic chip through interfacial polymerization[39].

Microdialysis was categorized by Song et al. in three different geometries: tubular, flat chip-like devices with sandwiched membranes and microdialysis probes[31]. Xu et al. demonstrated dialysis on a chip as an off- and online sample preparation method in 1998 with flowrates as low as of 2-5 μL/min[32], through a cellulose dialysis membrane which was clamped between two microfluidic chips. Buffer and analyte

Table 1 Specifications of the different microfluidic desalination techniques. The table contains dimensions of the microfluidic channel, the flowrate and the achieved amount of desalination.

	author, year	electrolyte	size sample channel height [µm]	width [µm]	flow rate [µL min⁻¹]	desalination
dialysis	Tibavinsky, T.A., 2015	100 mM KCl	6	100	0.5-2.5	95% in 1s
	Xu, N. ,1998	500 mM NaCl and 100 mM Tris and 10 mM EDTA	60	160	online 2-5 offline 0.01-0.3	online ESI SNR 40x improved
	Song, S., 2004	50 mM buffer 10ppm Rhodamine 560	20	280	0.01	30-80%
	Xiang, F., 1999	10 mM PBS	60	150	0.2-5	ESI SNR 20x improved
ED	Kwak, R., 2013	10 mM NaCl and 0.01 mM Rhodamine 6G	200	1000	10	90%
Shock ED	Deng, D., 2015	$2 \cdot 10^{-5}$ g mL⁻¹ Rhod. B in 1mM $CuSO_4$ 1 mg mL⁻¹ fluorescein in 1 mM $CuSO_4$	cylinder height 3000 and radius 5000		0.1-100	88% of neg. dye
ICP	Schiermeier, Q., 2008	seawater ≈ 500 mM	100	500		
	Kim, S., 2013	brackish water ≈ 100 mM	15	100	0.1-20	99%
	MacDonald, B.D., 2014	20, 200 and 500 mM NaCl	200	2000	0.5	90% for 500 mM
CDI	Suss, M.E., 2014	5-80 mM KCl	5000	1500	0	10% at t ≈ 25s
	Demirer, O., 2014	0.7 mM of fluorescein (-) and sulforhodamine B(+)	100	200	0	60% at t ≈ 60s
	Dak, P., 2014	<100 mM	droplet volume 50 pL		-	90%
	Roelofs, S.H., 2015	10 mM NaCl	400	1500	1	10% at t ≈ 3 min
ECD	Knust, K.N., 2013	seawater	22	100	0.08	25±5%
	Grygolowicz-Pawlak, 2012	0.6 M NaCl	cylinder length 480 mm	30	max 40	flow injection mode 90% in 90s

are separated by the membrane and the system is operated in counter flow. The buffer flowrate was 100 μL min⁻¹. The signal-to-noise ratio (SNR) of the ESI-MS spectrum was improved by a factor of 40 compared to the ESI-MS spectrum of the original sample containing salt, a specific desalination percentage is not mentioned. Xiang et al. performed online dual microdialysis which incorporated two membranes with different MWCOs[33]. The chip was coupled to ESI-MS, through an integrated spray-tip, and resulted in an improved SNR by a factor of 20. Song et al. increased the speed and introduced a photo-patterning method to implement dialysis membranes on a chip, with a desalination time of approximately 1 min[31,38].

Further increase in speed of dialysis on-chip for mass spectrometry purposes was demonstrated by Tibavinsky et al[38], who miniaturized a dialysis configuration and achieved a desalination percentage of 95% in 1s. The flowrate of the sample channel was 30-150 μL/h while the flowrate of the buffer channel was 50 mL/h, resulting is a recovery rate < 0.3% The pore size in these experiments was estimated at $\approx$ 50 nm[38]. They hypothesized that the diffusion time through the membrane is the most time consuming part of the process and reduced this through replacing the standard cellulose material with ultrathin alumina[38].

Drawbacks of dialysis are that besides the salt also part of the compounds of interest diffuse through the membrane into the buffer, which could result in a lower sensitivity of the analysis. The application of a membrane with a certain mechanical stability sets limits for the pressure difference and thus flowrate that can be applied.

4.2 Electrodialysis

4.2.0.1 Electrodialysis. The previously introduced macroscopic desalination technique electrodialysis was introduced on-chip in 2013[40]. Fig. 1b illustrates the configuration of a single cell electrodialysis setup. Two electrodes with a cat- and anion exchange membrane in between are placed in parallel. The elements are separated through spacers. A potential is applied across the stack which is sufficient to induce a Faradaic current. The ions in the electrolyte, entering from below, transport through the membranes. Cations can only pass through the cation selective membranes (CEM), whereas anions can only pass through anion selective membranes (AEM). This results in alternating dilute and concentrated streams, where the desalination percentage depends on the applied potential, the input concentration and the flowrate[27]. Strathmann reviewed electrodialysis and related processes in 2005[27]. Applications for electrodialysis are water desalination and salt pre-concentration[27]. Electrodialysis is currently not competitive with reverse osmosis in terms of energy efficiency. However, ED is a scalable technique, which does not require high pressure pumps as e.g. is required for RO[40], and can therefore be advantageous for applications where ion specificity or a high purity is required[27,40]. For the operational mode of an ED system three regimes, depending on the potential applied, can be distinguished: an Ohmic, limiting and over-limiting regime[41]. Fig. 3 illustrates these three regimes in a graph of the applied potential across an ED system versus the resulting current. In the Ohmic regime, 0-2 V, the applied potential and the resulting Faradaic current are linearly related. Upon the complete depletion of ions at the membrane surface, the limiting current is reached[27]. The mechanism behind the over-limiting current (OLC) is thus far explained as partly electroconvection[27,41], which is transport of volume due to migration
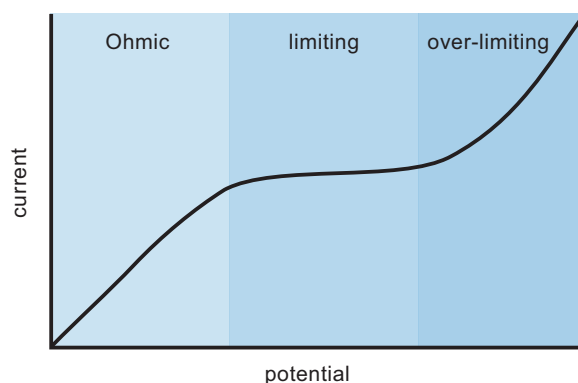

Fig. 3 Graph explaining the three operation regimes of electrodialysis: Ohmic, limiting and over-limiting, modified from Strathmann[27].

of charge present in the solution in the presence of an electric field[42] as well as water-splitting at or charge-carriers[42–44] and occurs at AEM[44,45]. An elaborate overview of theoretical and experimental work on electroconvection is given by Nikonenko[42]. Rubinstein et al. concluded from numerical studies and experiments with modified membranes that in addition to electroconvection, the electro-osmotic flow contributes to the over-limiting current[46].

Miniaturizing electrodialysis may contribute to optimization of the operation of large scale ED systems, through a thorough understanding of transport mechanisms. Kwak et al. investigated ion transport within an poldimethylsiloxane (PDMS) ED cell[40]. A 10 mM NaCl solution was inserted into the system. The local salt concentration as well as the flow profile was visualized through the addition of Rhodamine 6G which is positively charged[40]. With this platform experiments were performed in all three regimes. From their experiments they found that the observed asymmetry in the vortices at the AEM and CEM could be explained by different Stokes radii and transport properties of the cat- and anions[40]. Also the limiting regime for the CEM and AEM were reached at different potentials. They concluded that the optimal operation mode in terms of energy efficiency is the beginning of the over-limiting regime. The previous example illustrates that ED on-chip contributes to the fundamental understanding of ion transport near ion selective membranes and potentially leads to improvements of the energy efficiency of large-scale ED systems.

4.2.0.2 Shock electrodialysis. Deng et al. introduced a variation of ED named "shock electrodialysis", which in contrast to ED is not limited in speed by diffusion[47]. The operational principle is based on a porous frit (500 nm mean pore size), placed on top of a CEM (nafion) with a fluid reservoir located above these two layers. A potential of 0-2 V is applied,

which drives the system through the three regimes (Ohmic, limiting and over-limiting). The mechanism behind the over-limiting current in microchannels is explained by electroosmotic flow (EOF) or surface conduction (SC)[48]. For larger pores, with increased width, EOF is the dominant mechanism. The term "shock" refers to the sharp edge between the depletion region and the bulk electrolyte in the frit. It was demonstrated that desalted water could be removed from the reservoir. Shock ED may be applied to selectively remove ions by size or valence[47], for example to remove heavy metals. An alternative application for macro-scale shock ED is the treatment of produced water, which is a waste product from the oil and gas industry. Initial experiments demonstrated a decrease in concentration by 4 orders of magnitude[47]. In 2015 Deng et al. demonstrated additional benefits of the system, namely ion separation, disinfection and filtration on top of the earlier demonstrated desalination[49]. The combination of these properties make shock ED a candidate for compact systems.

4.3 Capacitive deionization

Capacitive deionization (CDI) is an electrostatic desalination technique which is potentially energy efficient for desalination of brackish water and waste-water streams from industry. Large-scale capacitive deionization in comparison to alternative desalination techniques was recently reviewed by Anderson and coworkers[18] and AlMarzooqi and coworkers[28]. An extensive review on the theory of CDI was published by Porada et al.[10]. A schematic overview of a CDI cell is shown in Fig. 2c. A typical CDI cell consists of two electrodes facing each other with an electrolyte flowing in between. To remove ions from the electrolyte solution, a potential of approximately 1 V is applied across two porous electrodes. The ions move to the oppositely charged electrodes and are stored in the electrical double layer. The storage capacity of the system is proportional to the effective surface area of the electrodes and the potential applied across the electrodes. During charging of the CDI cell, the applied potential and thus electron displacement is responsible for the removal of ions from the solution. At the same time co-ions are repelled from the electrodes, which results in an efficiency loss. The ratio between the amount of salt removed and the charge stored is defined as the charge efficiency and depends on the concentration and the applied potential[50–52]. To achieve desalination a charge efficiency $> 50\%$ is required, typical values are 65-70% for CDI with porous activated carbon electrodes[52]. A CDI system acts as an energy storage system which is equivalent in operational mechanism as a supercapacitor. For energy efficient operation the stored energy during charging should be regained during regeneration. According to Anderson et al. the energy consumption to produce a solution of 0.3 g L^{-1} is $\approx$ 0.3-1.9 kWh m^{-3} for an input concentration of 10 g L^{-1}, assuming a round

trip efficiency of 85%. The roundtrip efficiency is defined as the ratio between the energy retrieved during discharging vs. the energy input during charging. Water recovery rates of 78-86% have been observed, but strongly depend on the desired output concentration[53]. Implementing CDI on an optically transparent microfluidic chip enables the visualization of ionic transport through fluorescence microscopy. Suss and coworkers studied the spatially and temporally resolved salt concentration upon charging of a CDI cell[54]. Their experimental work was based on adding a neutral dye to the electrolyte, whose fluorescence intensity quenches upon colliding with a chloride ion. This resulted in the observation of two timescales, namely a quick cell charging process and a slower rate of desalination of the bulk. An alternative approach was used by Demirer and coworkers, who used laser induced fluorescence in a CDI cell with semi-porous electrodes[55]. They studied the transport of the charged fluorescent dyes using concentrations in the μM-range. We have experimentally and computationally demonstrated the formation of pH waves in a two electrode cell on-chip using fluorescence microscopy[56]. Recently we implemented CDI on-chip using porous carbon electrodes and demonstrated in situ impedance spectroscopy to monitor the average salt concentration between the desalination electrodes in real-time[57]. A two-electrode configuration
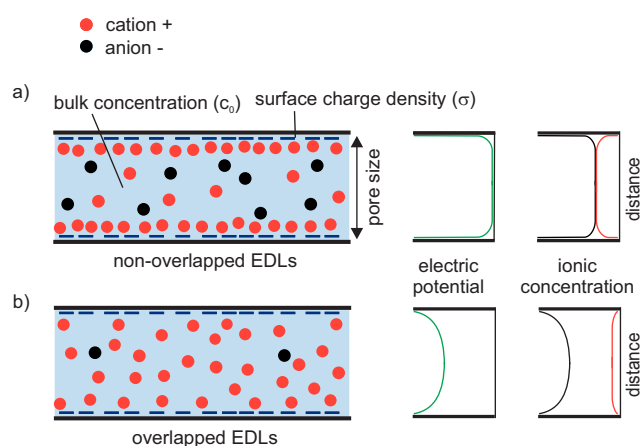
Fig. 4 a) Pore with non-overlapping double layers. b) Pore where double layer overlap takes place. Adapted with permission from Karnik et al.[14] Copyright (2005) American Chemical Society

to desalinate droplets was suggested by Dak and coworkers[58]. Their theoretical model based on the Poisson equation demonstrates that the bulk concentration of a 50 pL droplet with a starting sub-mM concentration can be desalinated substantially. Improvement of the performance is suggested through the use of fractal electrodes.

4.4 Ion concentration polarization

Ion concentration polarization (ICP) is a microfluidic desalination technique which was applied to desalinate seawater to fresh water by Kim and coworkers, as shown in Fig. 2d[29]. The operational mechanism of ICP can be explained in the following way. A current through an ion selective membrane establishes an ion depletion zone on one side of a membrane with pores of the size of approximately the Debye length[59]. The depletion zone occurs due to the fact that ions of similar charge at the walls of the nanopores present in the membrane are repelled by the membrane. The ions of opposite charge travel through the membrane pores. The result is an ion depletion zone on one side of the membrane and an ion enrichment zone on the other side of the membrane. This principle is applied by Kim et al.[29] to desalinate water using a y-shaped microfluidic channel, as depicted in Fig.2c. By passing a salt solution through the feed channel with a nanojunction located at the onset of the outlets, a desalted stream can be separated from a brine stream[29]. The nanojunction is a nanometer sized channel or pore which connects two larger, micrometer size channels[29]. Across the nanochannel a potential is applied and consequently, according to the above described operational mechanism, a depletion zone establishes at the interface between the nano- and microfluidic channel. The result is a fresh water stream exiting at one outlet and a concentrated brine solution exiting at the second outlet. ICP can be implemented to remove charge from uncharged species and not to separate particles/ions on the base of their mobility. The geometry is robust since separation is based on ions which are deviated from the membrane or nanopore away and not through the pores. ICP is scalable in sample throughput as was demonstrated by MacDonald et al.[60]. The energy consumption of the device was 4.6 and 13.8 Wh L^{-1} for 20 and 200 mM electrolyte, respectively[60]. The water recovery rate observed by Kim et al. was 50% at a salt rejection rate of 99%[29].

4.5 Electrochemical desalination

In contrast to previously discussed methods, electrochemical desalination (ECD) is based on Faradaic reactions occurring at electrodes upon a sufficiently high driving potential. By applying a potential of 3 V across a bipolar electrode, fabricated from pyrolyzed photoresist, the Cl$^-$ present in seawater oxidizes at the anode and neutralizes. The result is a local depletion zone. This phenomena is used by Crooks[61] and coworkers in a similar configuration that Kim and coworkers[29] used a nanopore for ICP to desalinate seawater. The reported rejection rate was 25$\pm$5% of salt. While the energy consumption was 25 mWhL^{-1} at a water recovery of 50%. The system is potentially energy efficient for small scale desalination facilities.

A cylindrical two-electrode electrochemical desalination cell was implemented by Grygolowicz et al.[30]. The center of the cylinder consists of a silver/silver chloride (Ag/AgCl) electrode. This is encapsulated by a nafion membrane which is again surrounded by a solution. Upon the application of a positive potential Cl$^-$ ions are removed from a sample solution through the oxidation of silver at the Ag/AgCl electrode which results in silver chloride formation. The nafion membrane is cation-selective and only passes the Na$^+$ ions while the transport of chloride ions is blocked[30]. It was demonstrated that in flow-through mode 90% of the salt is removed in 90 s with a maximum flowrate of 40 μL min^{-1} and start concentration of 0.6 M NaCl.

5 Field deployment of microfluidic based desalination systems

As stated in the introduction, the world wide fresh water demand is rising enormously and triggers the interest in new energy efficient desalination methods. In table 2 for each microfluidic desalination technique suitable applications are mentioned, however this section provides a more detailed discussion on the field deployment of each of the techniques. The water recovery rate of dialysis on-chip is only 0.3%, which is too low to consider dialysis as a large scale desalination technique. ED is a mature technology, which is due to its potential ion selectivity suitable for high purity applications. CDI is a potentially energy-efficient technique for desalination of brackish water with a high water recovery rate ($\approx$ 78-86%). For a competitive energy consumption rate per produced liter recovery of the stored energy in the system during charging is required[18]. In field prototype testing of a CDI device was already performed by Zhang et al.[62] and commercialization is on the verge of taking place by companies such as Voltea[63]. In contrast to the previously discussed techniques ICP is a young technology which was first introduced on chip in 2010 by Kim et al.[29,64]. The energy efficiency of a first demonstration of a scalable ICP device was a factor 10 lower than the reported energy efficiency of a CDI device with a realistic energy recovery percentage[53]. The water recovery percentage of electrochemical desalination is comparable to that of CDI and ICP and energy efficient operation was demonstrated for seawater desalination. Both ICP and electrochemical desalination are in an early development/research stage and the long-term stability of the processes requires further investigation.

6 Bridging the flow rate between macro and micro desalination systems

A hurdle in implementing microfluidic desalination techniques for macroscale desalination is scaling the flow rate of a

single chip, which is typically several μL min^{-1} or milliliter per day to a flow rate which could provide drinking water for a single person, family or village (liters to several hundreds of liters per day). The most simplistic idea is to implement several desalination units on a single chip via a single in-and outlet and to design stackable chips. Assuming a drinking water production flow rate of 5 μL min^{-1} and a drinking water consumption of 3 L per day for a single person, 416 chips are required to provide for a single person. The unit would cover a total volume of ≈ 0.25 liters. MacDonald et al. introduced the term "out-of-plane design" to describe their elegant approach to scale the desalination capacity of ICP on chip[60]. By extending the design in a third dimension the production capacity per volume is potentially higher. These creative design considerations are necessary to implement microfluidic desalination techniques for macroscale applications.

7 Summary and conclusion

7.1 Techniques

The microfluidic approach to desalination offers several advantages over macrofluidic desalination. The operational parameters of a microfluidic cell can be controlled in a precise manner and a microfluidic platform is perfectly suitable for monitoring the performance of the system electrochemically or in situ via fluorescence microscopy. Using micro- and nano fabrication methods new ion transport phenomena, such as ICP and shock ED are discovered and applied for desalination. Additionally, desalination on-chip can be integrated with complementary on-chip techniques for applications like biological sample preparation.

7.2 Applications

Microfluidic desalination has proven it's relevance for at least three application categories: first, as a platform to increase fundamental knowledge of ion transport on the nano- and microfluidic scale. In addition to early experimental methods, which were limited to electro(chemical) analysis at the in- and outlet of desalination system such as CDI[18,65–69], in-situ measurements using fluorescence microscopy can visualize ion transport, local salt concentration and flow profiles. This information is crucial to optimize macro-scale desalination systems. An example is the implementation of ED on-chip by Kwak et al.[40] who studied the optimal operation mode of ED in terms of energy efficiency. CDI on-chip was performed by Suss et al.[54] and Demirer et al.[55] who investigated charging behavior of the cell. Challenging systems requiring high pressures (RO) or high temperatures (MSF or MED) have not been applied on-chip yet and are most commonly implemented for large scale desalination.

Second, microfluidic desalination is a promising sample preparation technique, which enables the use of extremely small sample volumes in the nano- and picoliter range. It increases the speed of the sample preparation process, enhances the sensitivity of detection limits and can be integrated with other microfluidic sample preparation techniques. An example is the integration of dialysis on-chip as a sample preparation method for ESI-MS, which improves the SNR of ESI-MS spectra[32,33,38].

Third: new techniques, such as ICP, BPE and shock ED arise from the micro/nanofluidic approach to desalination and are promising techniques for scaling out to a size-range from portable to container-size desalination facility. Depending on factors like the input concentration (seawater or brackish water) and required purity, ICP[29,60] and ECD[61] are energy competitive to state-of-the art macro-scale techniques (RO, MSF and MED). Additionally these techniques do not suffer from membrane fouling.

References

1 M. Shannon, P. Bohn, M. Elimelech, J. Georgiadis, B. Maras and A. Mayes, *Nature*, 2008, **452**, 301–310.

2 A. Khawaji, I. Kutubkhanah and J.-M. Wie, *Desalination*, 2008, **221**, 47–69.

3 N. Ghaffour, T. M. Missimer and G. L. Amy, *Desalination*, 2013, **309**, 197 – 207.

4 M. Rogeberg, H. Malerod, H. Roberg-Larsen, C. Aass and S. Wilson, *Journal of Pharmaceutical and Biomedical Analysis*, 2014, **87**, 120–129.

5 R. Ramautar, G. Somsen and G. de Jong, *Electrophoresis*, 2014, **35**, 128–137.

6 S. Fekete, J. Schappler, J.-L. Veuthey and D. Guillarme, *TrAC - Trends in Analytical Chemistry*, 2014, **63**, 2–13.

7 J. Quist, P. Vulto and T. Hankemeier, *Analytical Chemistry*, 2014, **86**, 4078–4087.

8 A. M. Johnson, A. W. Venolia, R. G. Wilbourne, J. Newman, S. Johnson and R. H. Horowitz, *The electrosorb process for desalting water*, United Stated Department of the Interior Research and development progress report 516, 1970.

9 R. Burt, G. Birkett and X. S. Zhao, *Phys. Chem. Chem. Phys.*, 2014, **16**, 6519–6538.

10 S. Porada, R. Zhao, A. Van Der Wal, V. Presser and P. Biesheuvel, *Progress in Materials Science*, 2013, **58**, 1388–1442.

11 H. Helmholtz, *Annalen der physik und chemie*, 1879, **243**, 337–382.

12 D. Chapman, *Philos. Mag*, 1913, **25**, 475–481.

13 O. Stern, *Zeitschrift für elektrochemie und angewandte physikalische chemie*, 1924, **30**, 508–516.

14 R. Karnik, R. Fan, M. Yue, D. Li, P. Yang and A. Majumdar, *Nano Letters*, 2005, **5**, 943–948.

15 T. Zangle, A. Mani and J. Santiago, *Chemical Society Reviews*, 2010, **39**, 1014–1035.

16 K. Nijmeijer and S. Metz, *Sustainable Water for the Future: Water Recycling versus Desalination*, Elsevier, 2010, vol. 2, pp. 95 – 139.

17 J. O. Bockris, *Modern electrochemistry*, Kluwer Academic Publishers, 2nd edn, 2002, vol. 1.

18 M. Anderson, A. Cudero and J. Palma, *Electrochimica Acta*, 2010, **55**, 3845–3856.

19 *National oceanographic data center*, http://www.nodc.noaa.gov/, Accessed:2014-12-15.

20 NGWA, *Brackish ground water*, National ground water association (ngwa) brief, 2010.

21 Meeting the MDG drinking-water and sanitation target A mid-term assessment of progress, Geneva, 2004.

22 M. Elimelech and W. Phillip, *Science*, 2011, **333**, 712–717.

23 Q. Schiermeier, *Nature*, 2008, **452**, 260–267.

24 *Fumatech*, http://www.fumatech.com/EN/Membrane-technology/Membrane-processes/Electrodialysis/, Accessed:2015-02-16.

25 *Fumatech*, http://www.fumatech.com/EN/Membrane-technology/Membrane-processes/Reverse-osmosis/, Accessed:2015-02-16.

26 L. F. Greenlee, D. F. Lawler, B. D. Freeman, B. Marrot and P. Moulin, *Water Research*, 2009, **43**, 2317 – 2348.

27 H. Strathmann, *Desalination*, 2010, **264**, 268–288.

28 F. AlMarzooqi, A. Al Ghaferi, I. Saadat and N. Hilal, *Desalination*, 2014, **342**, 3–15.

29 S. Kim, S. Ko, K. Kang and J. Han, *Nature Nanotechnology*, 2010, **5**, 297–301.

30 E. Grygolowicz-Pawlak, M. Sohail, M. Pawlak, B. Neel, A. Shvarev, R. de Marco and E. Bakker, *Analytical Chemistry*, 2012, **84**, 6158–6165.

31 S. Song, A. K. Singh, T. J. Shepodd and B. J. Kirby, *Analytical Chemistry*, 2004, **76**, 2367–2373.

32 N. Xu, Y. Lin, S. A. Hofstadler, D. Matson, C. J. Call and R. D. Smith, *Analytical Chemistry*, 1998, **70**, 3553–3556.

33 F. Xiang, Y. Lin, J. Wen, D. Matson and R. Smith, *Analytical Chemistry*, 1999, **71**, 1485–1490.

34 D. Gao, H. Liu, Y. Jiang and J.-M. Lin, *Lab Chip*, 2013, **13**, 3309–3322.

35 A. E. Ashcroft, *Nat. Prod. Rep.*, 2003, **20**, 202–215.

36 N. Lion, V. Gobry, H. Jensen, J. S. Rossier and H. Girault, *Electrophoresis*, 2002, **23**, 3583–3588.

37 Y. Chen, M. Mori, A. C. Pastusek, K. A. Schug and P. K. Dasgupta, *Analytical Chemistry*, 2011, **83**, 1015–1021.

38 I. A. Tibavinsky, P. A. Kottke and A. G. Fedorov, *Analytical Chemistry*, 2015, **87**, 351–356.

39 Y. Zhang, N. E. Benes and R. G. H. Lammertink, *Lab Chip*, 2015, **15**, 575–580.

40 R. Kwak, G. Guan, W. Peng and J. Han, *Desalination*, 2013, **308**, 138–146.

41 R. Ibanez, D. Stamatialis and M. Wessling, *Journal of Membrane Science*, 2004, **239**, 119 – 128.

42 V. Nikonenko, A. Kovalenko, M. Urtenov, N. Pismenskaya, J. Han, P. Sistat and G. Pourcelly, *Desalination*, 2014, **342**, 85–106.

43 I. Rubinstein, E. Staude and O. Kedem, *Desalination*, 1988, **69**, 101–114.

44 I. Rubinstein, A. Warshawsky, L. Schechtman and O. Kedem, *Desalination*, 1984, **51**, 55–60.

45 R. Simons, *Desalination*, 1979, **28**, 41 – 42.

46 I. Rubinstein and B. Zaltzman, *Journal of Fluid Mechanics*, 2013, **728**, 239–278.

47 D. Deng, E. Dydek, J.-H. Han, S. Schlumpberger, A. Mani, B. Zaltzman and M. Bazant, *Langmuir*, 2013, **29**, 16167–16177.

48 E. Dydek, B. Zaltzman, I. Rubinstein, D. Deng, A. Mani and M. Bazant, *Physical Review Letters*, 2011, **107**, 118301.

49 D. Deng, W. Aouad, W. Braff, S. Schlumpberger, M. Suss and M. Bazant, *Desalination*, 2015, **357**, 77–83.

50 R. Zhao, P. Biesheuvel, H. Miedema, H. Bruning and A. van der Wal, *The Journal of Physical Chemistry Letters*, 2010, **1**, 205–210.

51 P. Dugoecki and A. Van Der Wal, *Environmental Science and Technology*, 2013, **47**, 4904–4910.

52 M. Mossad and L. Zou, *Chemical Engineering Journal*, 2013, **223**, 704 – 713.

53 C. Huyskens, J. Helsen and A. de Haan, *Desalination*, 2013, **328**, 8–16.

54 M. E. Suss, P. M. Biesheuvel, T. F. Baumann, M. Stadermann and J. G. Santiago, *Environmental Science & Technology*, 2014, **48**, 2008–2015.

55 O. Demirer and C. Hidrovo, *Microfluidics and Nanofluidics*, 2014, **16**, 109–122.

56 S. H. Roelofs, M. van Soestbergen, M. Odijk, J. C. T. Eijkel and A. van den Berg, *Ionics*, 2014, **20**, 1315–1322.

57 S. H. Roelofs, B. Kim, J. C. T. Eijkel, J. Han, A. van den Berg and M. Odijk, *Lab Chip*, 2015, **15**, 1458–1464.

58 P. Dak and M. Alam, Device Research Conference (DRC), 2014 72nd Annual, 2014, pp. 275–276.

59 S. J. Kim, Y.-A. Song and J. Han, *Chem. Soc. Rev.*, 2010, **39**, 912–922.

60 B. D. MacDonald, M. M. Gong, P. Zhang and D. Sinton, *Lab Chip*, 2014, **14**, 681–685.

61 K. N. Knust, D. Hlushkou, R. K. Anand, U. Tallarek and R. M. Crooks, *Angewandte Chemie International Edition*, 2013, **52**, 8107–8110.

62 W. Zhang, M. Mossad and L. Zou, *Desalination*, 2013, **320**, 80–85.

63 *Voltea*, www.voltea.com, Accessed: 2015-07-05.

64 S. Kim, S. Ko, K. Kang and J. Han, *Nature Nanotechnology*, 2013, **8**, 609.

65 T. Welgemoed and C. Schutte, *Desalination*, 2005, **183**, 327–340.

66 R. Zhao, M. van Soestbergen, H. Rijnaarts, A. van der Wal, M. Bazant and P. Biesheuvel, *Journal of Colloid and Interface Science*, 2012, **384**, 38–44.

67 A. M. Johnson and J. Newman, *Journal of The Electrochemical Society*, 1971, **118**, 510–517.

68 J. Farmer, D. Fix, G. Mack, R. Pekala and J. Poco, *Journal of the Electrochemical Society*, 1996, **143**, 159–169.

69 P. Biesheuvel and M. Bazant, *Physical Review E - Statistical, Nonlinear, and Soft Matter Physics*, 2010, **81**, 031502.

Table 2 This table gives a qualitative overview of each of the techniques, in which the applications, advantages as well as disadvantages of microfluidic desalination

	author	application	advantages	disadvantages
dialysis	Tibavinsky, T.A., 2015	ESI-MS	fast	loss of analyte flow rate too high for nano-ESI-MS
	Xu, N. ,1998	sample cleanup for ESI-MS DNA and protein samples	fast improved sensitivity ESI-MS	loss of analyte
	Song, S., 2004	enables analysis small volumes	on-chip membrane fabrication enables on-chip sample preparation	desalination time ≈ 1 min.
	Xiang, F., 1999	ESI-MS	reduced sample consumption low dead volume robust potential integration with other techniques	-
ED	Kwak, R., 2013	study and optimize ED process	in situ high water purity scalable	less energy-efficient than RO
Shock ED	Deng, D., 2015	seawater and brackish water desalination. potentially suitable for highly compact systems	bacteria are killed or filtered. filters micron scaled particles or aggregated nano-particles. separates positively from negatively charged particles	limited membrane fouling
ICP	Schiermeier, Q., 2008 Kim, S., 2013	small-scale or portable seawater desalination	potentially energy-efficient. low membrane fouling no high pressure pumps	energy-efficiency needs investigation no removal of neutral organic compounds
	MacDonald, B.D., 2014	portable water desalination	scalable cost-effective	-
CDI	Suss, M.E., 2014	CDI performance improvement study ion transport	in situ measurements spatially and temporally resolved	mm size range no flow
	Demirer, O., 2014	effect potential on bulk concentration study ion transport within electrodes	in situ measurements	electrodes are semi-porous, with large pores. no double layer overlap
	Dak, P., 2014	reduced temp DNA melting. improved sensitivity sensors. modulation of pH-profile e.g. isoelectric protein separation. control of electrolyte concentration in loc systems	increase in detection limit confined small volume	evaporation
	Roelofs, S.H. 2015	sample preparation demonstrated with desalination of FITC-dextran	in situ real-time concentration measurements increase in detection limit	optimization of speed and desalination percentage required
ECD	Knust, K.N., 2013	seawater desalination	no membrane low voltage operation low investment costs low pressure	life-time of the electrode is unknown
	Grygolowicz-Pawlak, 2012	seawater sample treatment for nutrient analysis through coulometry	full regeneration was achieved	operation in stop-flow regeneration is necessary